ISSN 1064-2269, Journal of Communications Technology and Electronics, 2017, Vol. 62, No. 7, pp. 780–787. © Pleiades Publishing, Inc., 2017.
Original Russian Text © V.A. Cherepenin, A.V. Zhuravlev, M.A. Chizh, A.V. Kokoshkin, V.A. Korotkov, K.V. Korotkov, E.P. Novichikhin, 2017, published in Radiotekhnika i Elektronika, 2017, Vol. 62, No. 7, pp. 672–680.

THEORY AND METHODS OF SIGNAL PROCESSING

Reconstruction of Subsurface Radio Holograms Fully and Partially Measured by Different Methods

V. A. Cherepenin[a], A. V. Zhuravlev[b], M. A. Chizh[b], A. V. Kokoshkin[c, *], V. A. Korotkov[c], K. V. Korotkov[c], and E. P. Novichikhin[c]

[a] *Kotel'nikov Institute of Radio Engineering and Electronics, Russian Academy of Sciences, Moscow, 125009 Russia*
[b] *Bauman State Technical University, Moscow, 105005 Russia*
[c] *Kotel'nikov Institute of Radio Engineering and Electronics (Fryazino Branch), Russian Academy of Sciences, Fryazino, Moscow oblast, 141120 Russia*
**e-mail: shvarts65@mail.ru*

Received March 14, 2016

Abstract—Reconstruction of measured holograms is performed by the backward propagation method and by means of a preliminary measured instrument function (IF). It is shown that the results of the reconstruction can be improved by reducing the IF measuring error, e.g., by averaging over a ring. It is established that images of a part of subsurface radio holograms can be obtained not only if the known part of a hologram is an entire fragment but also if the measured points of the hologram are not nearest neighbors of each other.

DOI: 10.1134/S1064226917070038

The obtainment and reconstruction of subsurface radio holograms is a topical issue in the field of detection, identification, and non-destructive testing of hidden objects.

Subsurface radio holograms are different from the common types of holograms (Fourier, Fresnel, Fraunhofer holograms, focused images) [1–9]. This distinction is caused by specific features of the measurement method (the source and the receiver of radiation are at the same point) and the conditions of measurements (due to a small distance, a part of the irradiated object can be situated beyond the main lobe of the radiation pattern of a transmitting–receiving antenna). Information on the properties of the transmitting–receiving antenna can be either used or not used by the imaging methods. In addition, such information can be used when reconstructing the image from the hologram as from an ordinary defocused image (without data on the phase of the received signal).

This work is devoted to the reconstruction of subsurface radio holograms fully or partially measured by different methods. The influence of irregularities of the layer on the quality of image reconstruction we will be neglected, since this influence was thoroughly studied in [4, 7, 10].

1. COMPARISON OF RECONSTRUCTION OF RADIO HOLOGRAMS BY THE BACKWARD PROPAGATION METHOD AND BY MEANS OF A MEASURES INSTRUMENT FUNCTION

Consider a method for reconstruction of radio holograms. Let a plane object parallel to the scanning plane be located at a distance z_0 from this plane (Fig. 1).

1.1. Backward Propagation Method

A signal $E(x, y)$ detected by the antenna receiver at each point of the scan plane can be expressed as the sum of the products of the signals reflected from each point of the object by a factor expressing the retardation of the reflected wave from a reference wave [3, 4]:

$$E(x,y) = \iint r(x',y') \times \exp\left(-i2k\sqrt{(x-x')^2 + (y-y')^2 + z_0^2}\right)dx'dy', \quad (1)$$

where $r(x', y')$ is the reflectance of an object (the ratio between the intensities of the reflected and incident

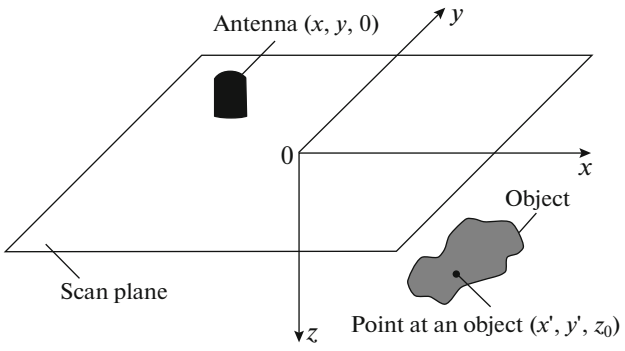

Fig. 1. Geometry of the holographic system.

waves), $k = 2\pi f/c$ is the wavenumber, f is the frequency of the scanning signal, and c is the speed of light. The factor 2 in the exponent is caused by the double travel path of the wave: from the antenna to the object and backward. This expression disregards the influence of the antenna directional pattern and the signal attenuation in the medium [2–4].

Carrying out the transformations described in [3, 4], we obtain the final expression used to reconstruct holograms:

$$r(x,y) = \Phi_{2D}^{-1}\left\{\Phi_{2D}\{E(x,y)\}\exp\left(2iz_0\sqrt{k^2 - k_x^2 - k_y^2}\right)\right\}. \quad (2)$$

Here, $\Phi_{2D}\{r(x,y)\}$ and $\Phi_{2D}^{-1}\{r(x,y)\}$ are the direct and inverse Fourier transforms:

$$\begin{aligned}\Phi_{2D}\{r(x,y)\} &= \iint r(x,y)\exp(-i(k_x x + k_y y))dxdy,\\ \Phi_{2D}^{-1}\{F(k_x,k_y)\} &= \iint F(k_x,k_y)\exp(i(k_x x + k_y y))dk_x dk_y.\end{aligned} \quad (3)$$

1.2. Solving the Problem by Means of the Instrument Function

In the framework of Huygens–Fresnel conceptions, the signal $E(x,y)$ detected by the antenna receiver at each point of the scan plane can be expressed as the sum of spherical waves reflected from each point of the object [2–4, 7–15]:

$$E(x,y) = \iint A(x - x', y - y')\, r(x', y')\, dx'dy', \quad (4)$$

where $A(x - x', y - y')$ is the instrument function (IF) of the measuring system, equal to the field measured at a point (x,y) from a point object having coordinates (x', y') and scattering the field of the irradiating antenna. In this case, the IF depends on the difference between the coordinates of the point object and the transmitting–receiving antenna, because the coordinates of the receiving and transmitting antennas in this problem coincide.

The solution to Eq. (4) with respect to $r(x', y')$ can be obtained be means of the Fourier transform:

$$r(x,y) = \Phi_{2D}^{-1}\{\Phi_{2D}\{E(x,y)\}/\Phi_{2D}\{A(x,y)\}\}. \quad (5)$$

Unfortunately, solution (4) in form (5) is unstable due to disturbances, noise, and errors of determining $A(x - x', y - y')$. The regularization of (5) can be performed on the basis of a simplified Wiener filter with a parameter equivalent to the ratio between the noise and signal spectral powers [2, 5, 6].

The IF can be determined using the measurement of the field scattered by a ball with a diameter smaller than the expected details of the scanned object.

1.3. Results of Reconstruction of Measured Holograms

All the experimental results used below were obtained at the Bauman Moscow State Technical University at a test bench working in the range of frequencies up to 24 GHz. The general view of the test bench is shown in Fig. 2; its detailed description is given in [3, 4, 7, 10–16].

The measuring part of the test bench includes a Rohde & Schwarz vector network analyzer and a transmitting–receiving antenna in the form of a circular open-end waveguide connected to it by flexible cables. The vector network analyzer plays the role of a generator of a continuous signal with a step-wise frequency variation. It enables one to detect both amplitude and phase of the signal reflected by the object by measuring the complex reflection coefficient S. The

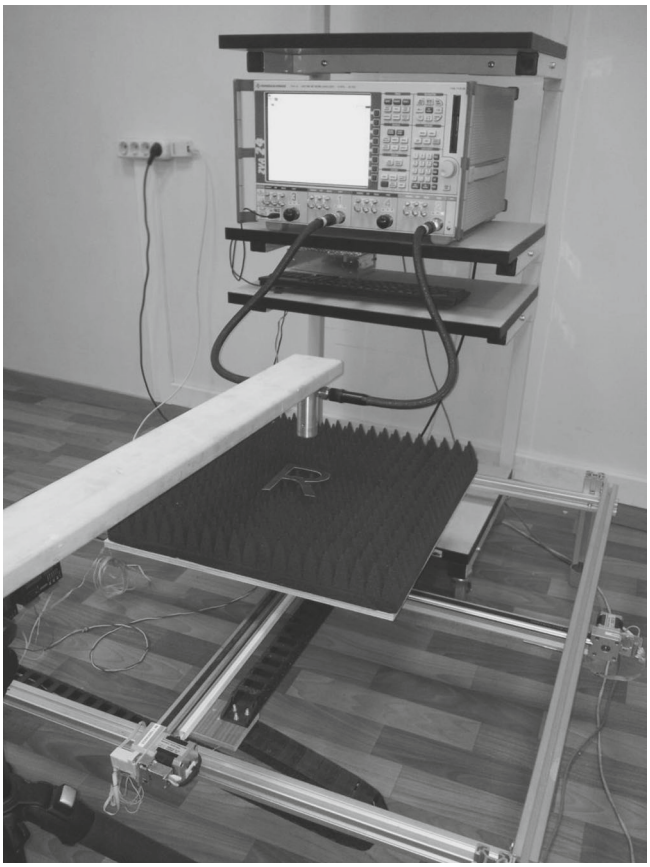

Fig. 2. General view of the test bench.

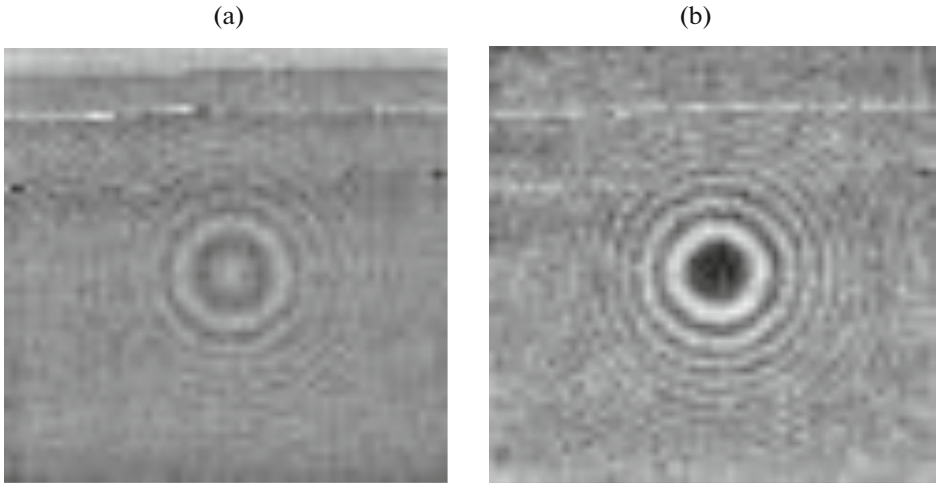

Fig. 3. The (a) real and (b) imaginary parts of the hologram of the measured field from a metal ball.

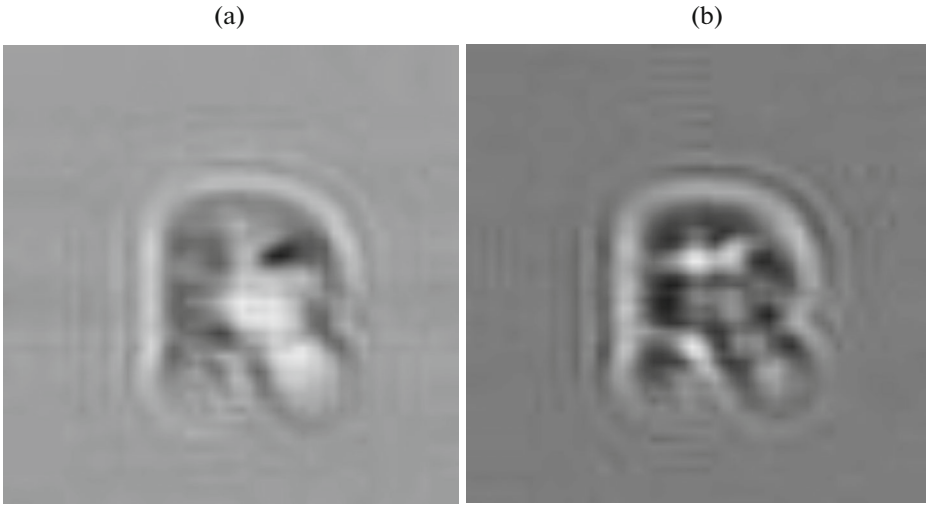

Fig. 4. The (a) real and (b) imaginary parts of the hologram of the measured field from object "R".

receiver is decoupled from the transmitter inside the vector analyzer. When measuring the *S*-parameters, the influence of the transmitter on the receiver is disregarded and compensated by the Rohde & Schwarz vector network analyzer. The antenna is fixed on an antenna holder, which enables one to adjust manually the height of the antenna above the scanned region. The scanning part of the test bench consists of two linear electromechanical scanners fixed on an aluminum frame. The scanners move the platform with the analyzed object near the antenna. The line-by-line movement of the platform makes it possible to synthesize the aperture: the field scattered by the object is measured automatically with a program-specified sampling frequency. For the real-time control of the stepper, the initiation of the frequency sweep on the vector analyzer, and the synchronization of the cycles of object's motion with measuring cycles, a microcontroller device connected to a personal computer was used. The computer software, developed in Python programming language, provides a command interface with a possibility to control the test bench and select various scan parameters, such as the area of the scanned region, the sampling rate, the bandwidth, and the difference between the frequencies of the signal emitted by the antenna.

To reconstruct holograms by means of the IF, measurements of the field scattered by a metal ball with a diameter of 8 mm were performed. The test samples comprised a metal letter "R" and a metal key. It should be noted that object "R" was placed at the same distance $z_0 = 0.105$ m as the metal ball. The measurement step $\mathrm{Step} = 0.005$ m for these objects was also the same. In object "key", these quantities were $z_0 = 0.04$ m and $\mathrm{Step} = 0.0036$ m, respectively.

Figure 3 shows the images of the hologram of a metal ball (the real and imaginary parts of the measured field). Figure 4 shows images of the hologram, and Fig. 5, images of object "R". The image in Fig. 5a was performed by the backward propagation method

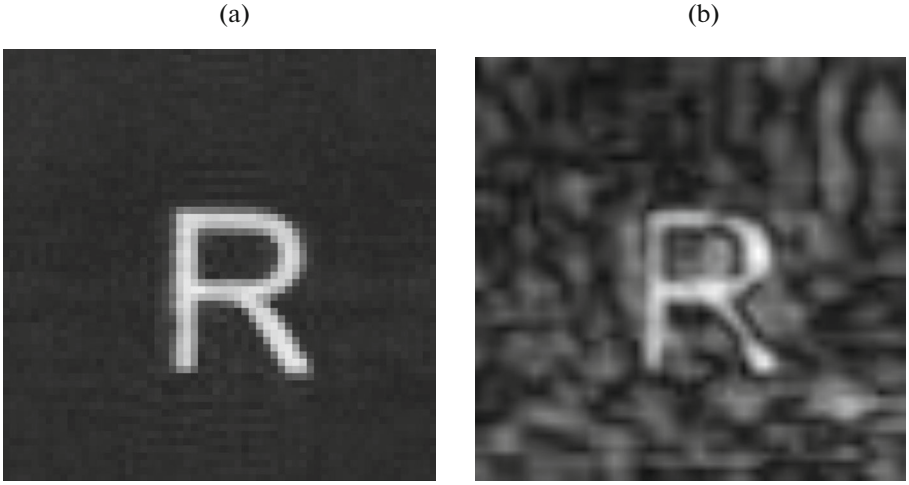

Fig. 5. Images of object "R" reconstructed by (a) BPM (3) and (b) by means of IF (5), shown in Fig. 3.

(BPM) (see formula (3)) and, in Fig. 5b, by means of the IF (see formula (5)). The measured IF is shown in Fig. 3.

In Fig. 5b, we see numerous artifacts not found in Fig. 5a. We may assume that they are caused by errors in measuring the field scattered by the metal ball, which was used as an IF. To reduce the influence of these errors, we average the field shown in Fig. 3 over a ring of unit width with the center located at the center of Fig. 3. The results of application of the field averaged over the ring as an IF are presented in Fig. 6. For comparison, Fig. 7 shows the results of reconstructing the hologram of object "key". Despite the fact that the holograms of this object and the ball for determining the IF were measured in different conditions, the reconstruction by means of the IF gives results comparable with BPMs.

Another interesting option for reconstructing a hologram by means of the IF is to use only the measured absolute value of the field both for the hologram of the object and the IF. In this case, the IF is equivalent to the scattering function of the point. Figure 8 illustrates exactly this case. It can be seen from the figure that the refusal of the phase part when reconstructing the hologram leads to an increase in the errors, which manifests itself in artifacts in the reconstructed image.

2. IMAGING OF A RADIO HOLOGRAM FROM ITS KNOWN PART

The obtainment of radio holograms requires a significant amount of measurements, which take a certain time. However, if the location of the object is known, the measurement of the hologram can be made in the spatial region containing the most part of information about the object. Therefore, obtaining an image from the measured part of a radio hologram is a pressing task. Subsurface radio holograms are different from optical holograms. Each point of a radio hologram contains information only about a part of the image, due to the influence of the directional pattern of the receiving–transmitting system. Since the wavelengths in this case are relatively large as compared to the case of optics, the field varies slowly from pixel to pixel. Therefore, a preliminary "outline" of the image from an incompletely measured hologram can be used to determine the location of the object of interest.

The measured part of a hologram may be (1) a half of the entire hologram, (2) a set of randomly arranged points, and (3) a set of randomly directed lines of mea-

Fig. 6. Image of object "R" reconstructed by means of IF (5). The role of the IF is played by the hologram in Fig. 3, averaged over a ring.

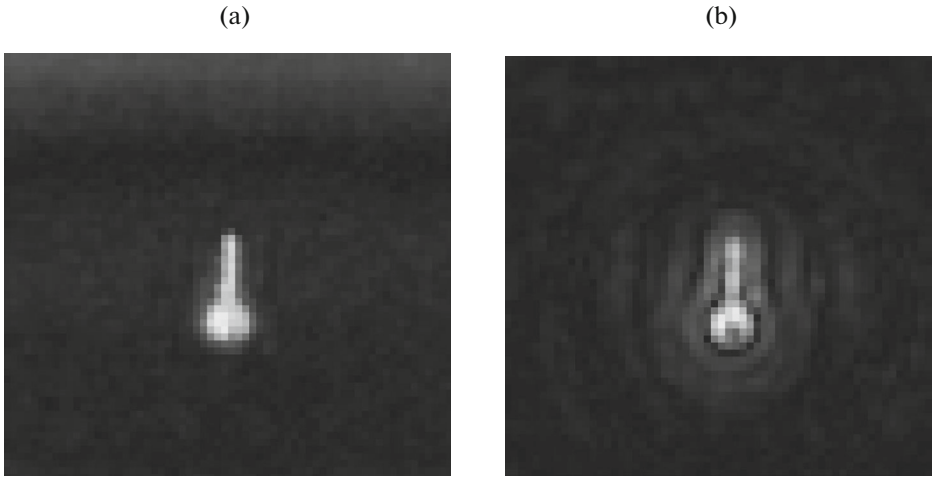

Fig. 7. Images of object "key" reconstructed (a) by BPM (by formula (3)) and (b) by means of IF (by formula (5)).

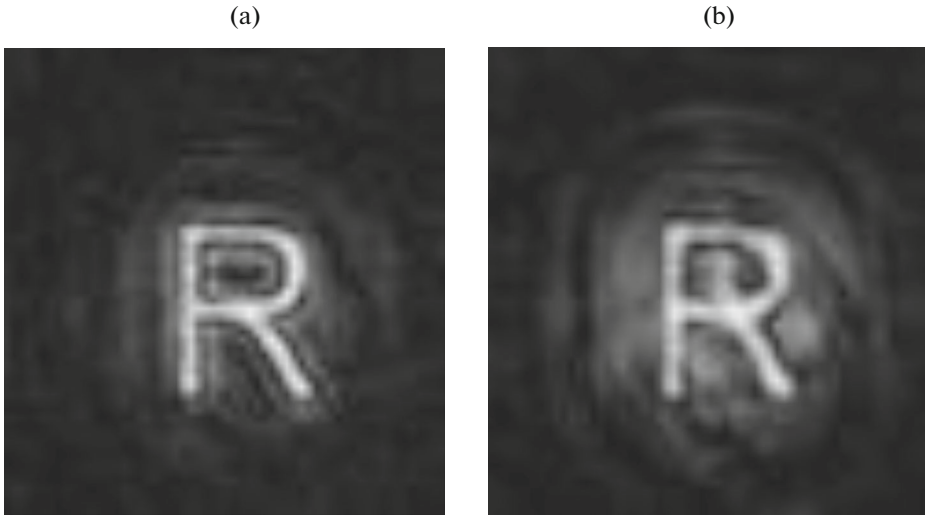

Fig. 8. Images obtained by means of an IF with using (a) complex values and (b) the absolute values of the field.

surements in which the origin of a current line coincides with the end of the previous line.

For example, Fig. 9 shows a measured hologram (real and imaginary parts) and an image calculated by the BPM. The hologram size is 74 × 74 or 5476 pixels.

2.1. Measuring the Upper Half of a Holograms

Let us consider the case of measuring only the upper half of a hologram. Figures 10a and 10b show examples of a measured half of the hologram obtained from Fig. 9. The calculated BPM image is shown in Fig. 10c.

This figure illustrates the fact that the upper half of a hologram contains information mainly about the upper half of the object and partially (as far as permitted by the beamwidth of the transmitting–receiving antenna) about the lower half.

2.2. Measuring a Hologram at Randomly Arranged Points

Consider the application of the BPM to measuring a hologram at randomly arranged points. Figures 11a and 11b show examples of a hologram obtained from Fig. 9, measured at randomly arranged points. The image calculated by the BPM is shown in Fig. 11c. Figures 11a and 11b contain only 900 pixels of the hologram in Fig. 9 or 15% of the total number of points. However, as will be shown below, this is sufficient to reconstruct the image.

2.3. Randomly Directed Lines of Measuring a Hologram

If the "measured" values of a hologram are arranged in the form of randomly directed measurement lines, the results are similar to those presented in Fig. 11 and are shown in Fig. 12. Figures 12a and 12b

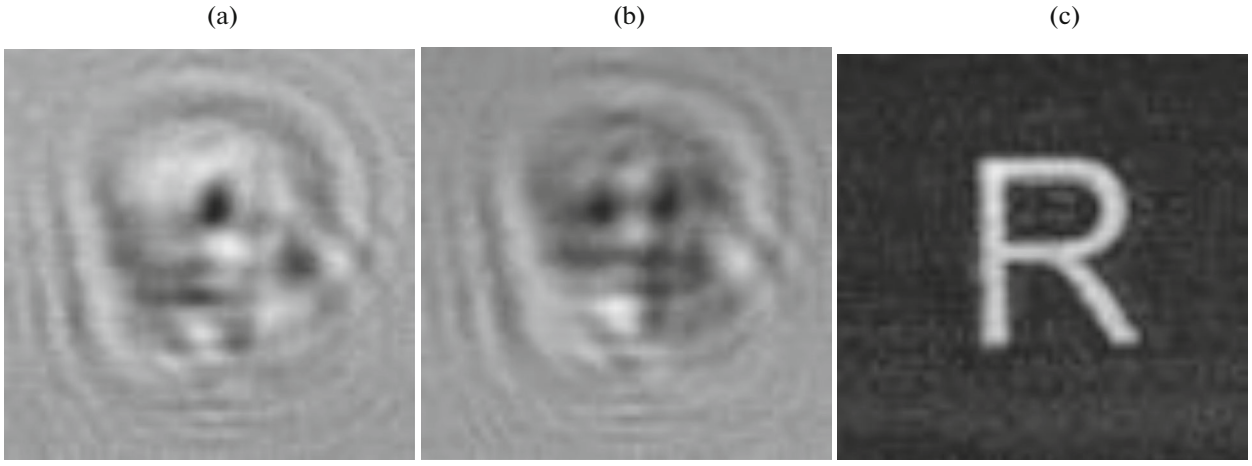

Fig. 9. The (a) real and (b) imaginary parts of the hologram of the measured field and (c) the image reconstructed by the BPM.

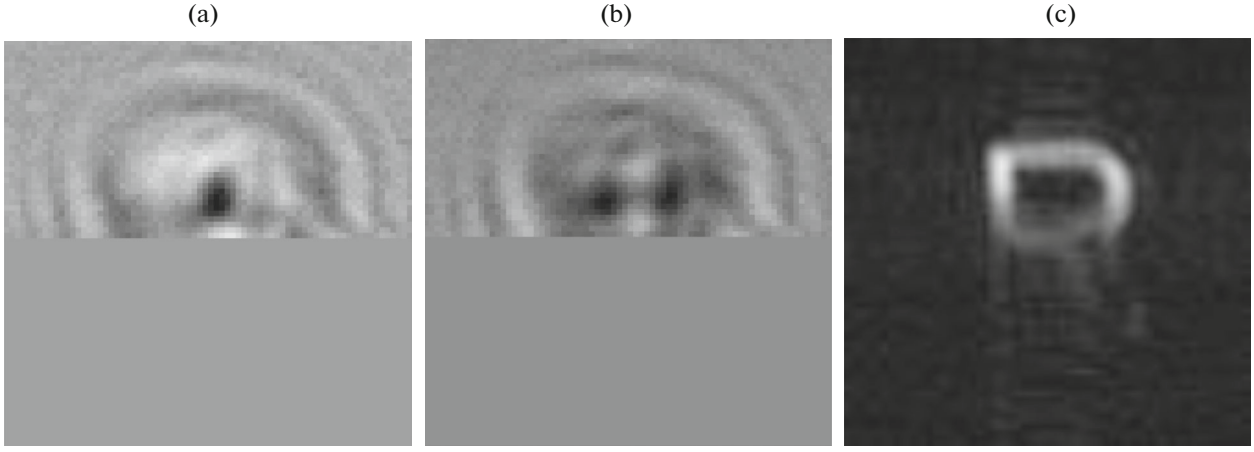

Fig. 10. The (a) real and (b) imaginary parts of the hologram of the measured field ("measured" in the upper half) and (c) the image reconstructed by the BPM.

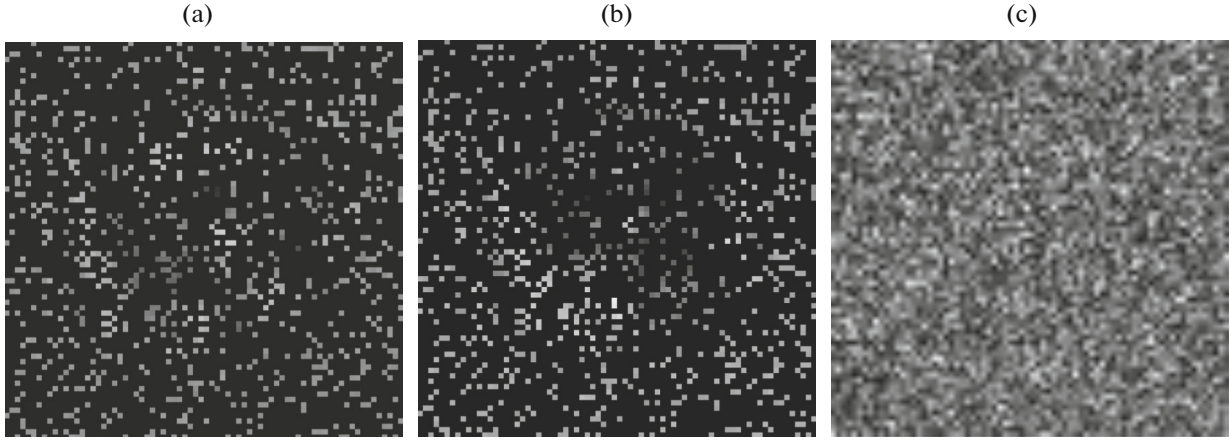

Fig. 11. The (a) real and (b) imaginary parts of a hologram of the measured field ("measured" at random points) and (c) the image reconstructed by the BPM.

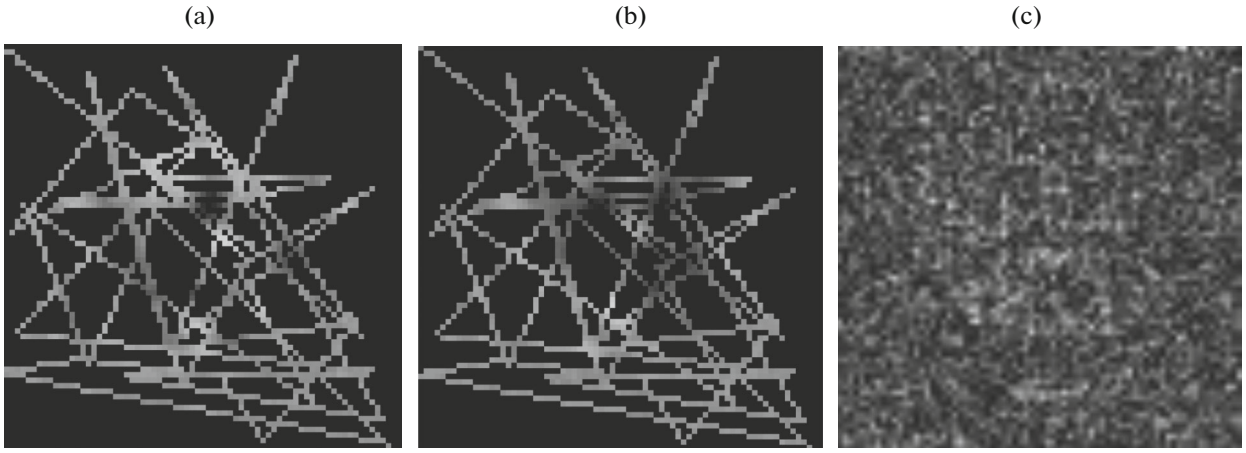

Fig. 12. The (a) real and (b) imaginary parts of the measured field ("measuresd on randomly directed lines) and (c) the image reconstructed by the BPM.

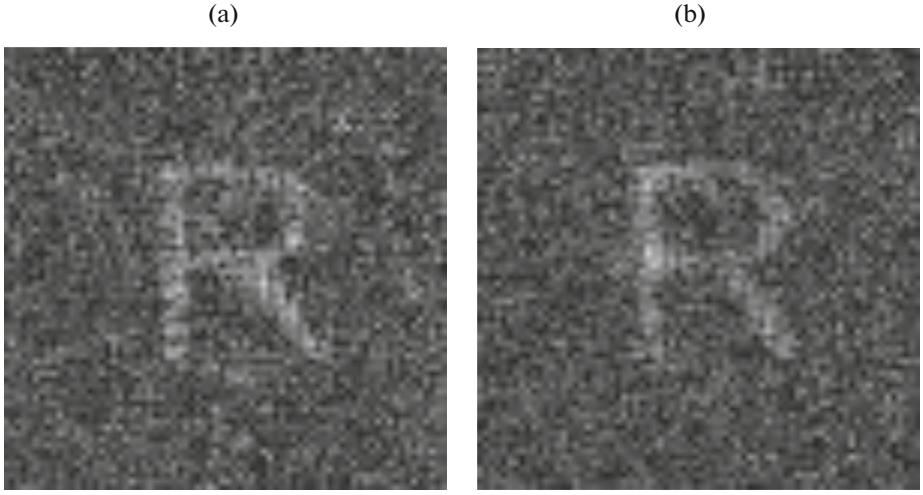

Fig. 13. Images calculated by the BPM, corresponding to (a) Fig. 11 and (b) Fig. 12 after assigning to "unmeasured" points the values averaged over the hologram.

contain 35 randomly directed measurement lines of random length with 1107 measured points or 20% of the total number of points.

2.4. Reconstructing Images of Incompletely Measured Holograms

As can be seen from Figs. 11c and 12c, in contrast to the case in Fig. 10c, the image from a part of the hologram has not been reconstructed. This result is explained by the presence of unmeasured points, visible in Figs. 11a, 11b, 12a, and 12b in the form of black dots (Figs. 10a, 10b) or regions of dots (Figs. 12a, 12b). However, the information in Figs. 11 and 12 is sufficient to obtain the image. To verify this, it suffices to replace the unmeasured (zero) values by the mean values for the corresponding part of the field. Figure 13 shows the results of image reconstruction after such a replacement.

The quality of the reconstructed images in Fig. 13 is approximately the same, since the proportion of "unmeasured" points in both holograms (see Figs. 11 and 12) is close to 15% and 20%, respectively. The noise clearly visible in Fig. 13 can be significantly reduced by replacing the "unmeasured" points in these figures (see Figs. 11a, 11b, 12a, and 12b) with the values interpolated from known "measured" points. The type of interpolation is not very important. This can be either linear, parabolic, or spline interpolation or the averaged values calculated from the nearest "measured" points. Applying interpolation by averaging to the holograms in Figs. 10 and 11, we obtain the result presented in Fig. 14.

The comparison between Fig. 9c and Figs. 14a and 14b leads us to the conclusion that the quality of reconstruction significantly increases due to the reduction of noise as a result of interpolation.

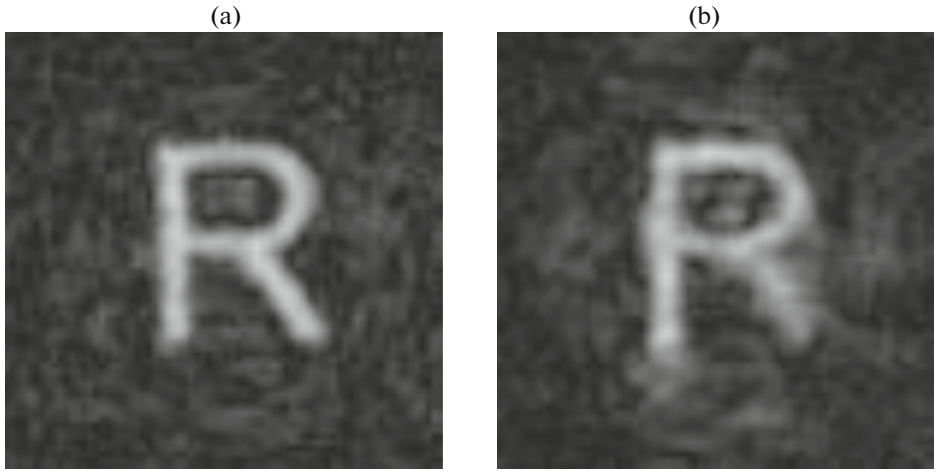

Fig. 14. Images calculated by the BPM, corresponding to (a) Fig. 11 and (b) Fig. 12 after assigning interpolated points to "unmeasured" points.

CONCLUSIONS

(1) Reconstruction of measured holograms is possible both by the backward propagation method and by means of a preliminary measured instrument function. Theoretically, these methods become equivalent when the IF is replaced with the phase part of a spherical wave.

(2) The errors of measuring the IF significantly affect the results of restoration. The results of restoration can be improved by reducing these errors, e.g., by averaging over a ring.

(3) Images of a part of subsurface radio holograms can be obtained not only when the known part of the hologram is an entire fragment but also if the measured points of the hologram are not the nearest neighbors of each other.

(4) Assigning to unmeasured points the values averaged over the hologram makes it possible to calculate the image. The noisiness of such an image depends on the fraction of measured points in the total number of points.

(5) The replacement of the mean values with interpolated values can significantly improve the quality of the image due to the reduction of noise.

ACKNOWLEDGMENTS

This work was supported by the Russian Science Foundation, project no. 15-19-30012.

REFERENCES

1. J. V. Goodman, *Introduction to Fourier Optics* (McGraw-Hill, New York, 2005).
2. R. C. Gonzalez and R. E. Woods, *Digital Image Processing* (Addison-Wesley, Reading, Mass., 1992; Tekhnosfera, Moscow, 2005).
3. A. V. Zhuravlev, S. I. Ivashov, V. V. Razevig, et al., in *Proc. 7th Int. Workshop on Advanced Ground Penetrating Radar (IWAGPR), Nantes, July 2–5, 2013* (IEEE, New York, 2013).
4. V. V. Razevig, A. S. Bugaev, and S. I. Ivashov, Usp. Sovrem. Radioelektron., No. 3, 3 (2012).
5. A. V. Kokoshkin, V. A. Korotkov, K. V. Korotkov, and E. P. Novichikhin, J. Radioelektron., No. 7 (2015); http://jre.cplire.ru/iso/jul15/4/text.pdf.
6. A. V. Kokoshkin, V. A. Korotkov, K. V. Korotkov, and E. P. Novichikhin, J. Radioelektron., No. 7 (2015); (http://jre.cplire.ru/iso/jul15/5/text.pdf).
7. A. Zhuravlev, S. Ivashov, V. Razevig, et al., Proc. SPIE—Int. Soc. Opt. Eng. **9072**, 90720X (2014).
8. L. P. Yaroslavskii and N. S. Merzlyakov, *Digital Holography* (Nauka, Moscow, 1982) [in Russian].
9. I. S. Klimenko, *Holography of Focused Images and Speckle-Interferometry* (Nauka, Moscow, 1985) [in Russian].
10. A. V. Zhuravlev, S. I. Ivashov, V. V. Razevig, et al., in *Proc. IET Int. Radar Conf., Xian, Apr. 14–16, 2013* (IEEE, New York, 2013), p. 6624275.
11. S. I. Ivashov, V. V. Razevig, I. A. Vasil'ev, et al., in *Radar and Radio Communication* (*Proc. 4th All-Russia Conf. Moscow, Nov. 29–Dec. 3, 2010)* (Informpress, Moscow, 2010), p. 89.
12. V. V. Razevig, S. I. Ivashov, I. A. Vasiliev, et al., in *Proc. XIII Int. Conf. on Ground Penetrating Radar, Lecce, June 21–25, 2010* (IEEE, New York, 2010), p. 657.
13. A. Zhuravlev, V. Razevig, M. Chizh, et al., in *Proc. 16th Int. Conf. of Ground Penetrating Radar 2016, Hong Kong, June 13–16, 2016* (IEEE, New York, 2016), p. 7572627.
14. V. V. Razevig, I. A. Vasil'ev, A. V. Zhuravlev, and S. I. Ivashov, in *Radars & Communications 3 (Proc. 3rd All-Russia Sci.-Eng. Conf., Moscow, Oct. 26–30, 2009)* (IRE RAN, Moscow, 2009), Vol. 1, p. 173.
15. V. V. Razevig, A. S. Bugaev, S. I. Ivashov et al., Usp. Sovrem. Radioelektron., No. 9, 51 (2010).
16. M. A. Chizh, A. V. Zhuravlev, V. V. Razevig, and S. I. Ivashov, in *Proc. Progress in Electromagn. Res. Symp. (PIERS 2016), Shanghai, Aug. 8–11, 2016* (IEEE, New York, 2016), p. 1734.

Translated by E. Chernokozhin